NANO LETTERS

2007
Vol. 7, No. 10
3106−3111

# Selective Surface Functionalization of Silicon Nanowires via Nanoscale Joule Heating

**Inkyu Park*,† Zhiyong Li,*,‡ Albert P. Pisano,† and R. Stanley Williams‡**

*Berkeley Sensor and Actuator Center (BSAC), University of California, Berkeley, California 94720-1774, and Quantum Science Research (QSR), Hewlett-Packard Laboratories, Palo Alto, California 94304*

*Received July 6, 2007; Revised Manuscript Received September 4, 2007*

## ABSTRACT

**In this letter, we report a novel approach to selectively functionalize the surface of silicon nanowires located on silicon-based substrates. This method is based upon highly localized nanoscale Joule heating along silicon nanowires under an applied electrical bias. Numerical simulation shows that a high-temperature (>800 K) with a large thermal gradient can be achieved by applying an appropriate electrical bias across silicon nanowires. This localized heating effect can be utilized to selectively ablate a protective polymer layer from a region of the chosen silicon nanowire. The exposed surface, with proper postprocessing, becomes available for surface functionalization with chemical linker molecules, such as 3-mercaptopropyltrimethoxysilanes, while the surrounding area is still protected by the chemically inert polymer layer. This approach is successfully demonstrated on silicon nanowire arrays fabricated on SOI wafers and visualized by selective attachment of gold nanoparticles.**

Recently, there have been great interest and active development in nanowire-based sensors. In particular, silicon nanowires (SiNWs) have been reported as sensors for the detection of solution pH level, protein,[1] gas molecules,[2] DNA,[3] cancer markers,[4] and neuron signals.[5] The sensing mechanism in those SiNW sensors is generally believed to be the change of their electrical conductance in the presence of charged chemical or biological molecules at their surface.[6] Because of the large surface-to-volume ratio and quasi-1D characteristics, SiNWs can be ultrahigh sensitivity sensors. For example, detection of fM levels of protein[4] and DNA[7] have been reported by using SiNWs. However, a SiNW itself has no chemical specificity toward analytes. To detect certain target species, the surfaces of SiNWs have to be functionalized with proper probe molecules that can interact with the specific target species to be detected. Moreover, selective functionalization of a SiNW array will be of great importance to render SiNW-based sensors versatile and practical. It can potentially improve the sensitivity and detection limit of the sensor by functionalizing SiNWs only while keeping the surrounding areas inert. Furthermore, multiplexed sensing will be made possible by functionalizing individual SiNWs with different probe molecules. There have been previous efforts to localize surface functionalization by electrostatic attraction of probe molecules on the electrodes,[8] photolithographic definition of a hydrophobic layer,[9] microcontact printing,[10] dip-pen nanolithography,[11] and electrochemical methods.[12] However, the electrostatic attraction scheme does not provide a great selectivity for surface modification against surrounding regions and also cannot be used for the attachment of neutral or weakly charged probe molecules. Photolithographic and microcontact printing methods cannot provide ultrafine localization in nanoscale dimensions. Furthermore, printing techniques also require precise alignment to the prefabricated micro/nanostructures. Dip-pen nanolithography provides an excellent design flexibility of selective surface functionalization and molecule binding but requires expensive equipment and does not provide a high-throughput surface functionalization. Electrochemical methods are restricted to the choice of functional groups, which require redox properties.

In this letter, we introduce an approach to achieve a selective surface functionalization of SiNWs. This method is based upon highly localized nanoscale Joule heating along SiNWs under applied electrical bias. Such localized heating is then utilized to selectively ablate a protective polymer layer on the chosen SiNW surface. The overall procedure of the selective surface functionalization by localized Joule heating is shown in Figure 1. First, a protective polymer layer is

* Corresponding authors. E-mail: Inkyu@eecs.berkeley.edu (I.P.); zhiyong.li@hp.com (Z.L.). Telephone: +1 510 643 1099 (I.P.); +1 650 236 4393 (Z.L.). Fax: +1 510 643 6637 (I.P.); +1 650 236 9885 (Z.L.). Addresses: 497 Cory Hall, Mailstop 1774, Berkeley Sensor and Actuator Center (BSAC), University of California, Berkeley, CA 94720-1774 (I.P.); Quantum Science Research (QSR), Hewlett-Packard Laboratories, 1501 Page Mill Road, Palo Alto, CA 94304 (Z.L.).

† Berkeley Sensor and Actuator Center (BSAC), University of California, Berkeley.

‡ Quantum Science Research (QSR), Hewlett-Packard Laboratories.

10.1021/nl071637k CCC: $37.00 
**Published on Web 09/26/2007**

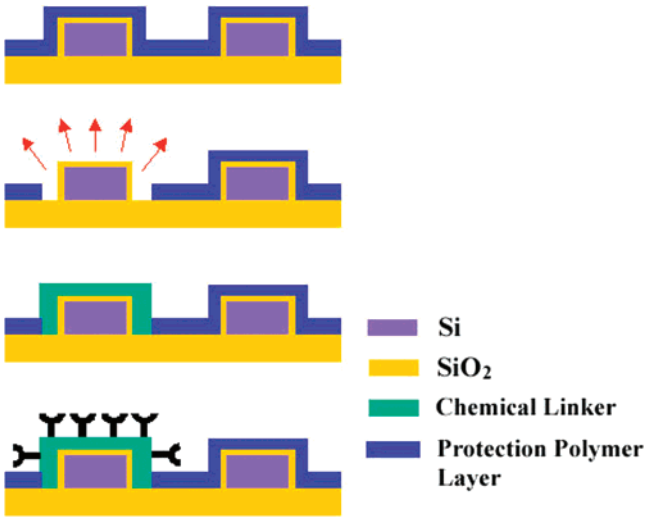


**Figure 1.** Process flow of the selective surface functionalization approach: (1) Deposit a uniform coating of inert polymer layer; (2) Joule heating of silicon micro/nanowire for localized ablation of polymer layer followed by low power $O_2$ plasma treatment; (3) Surface modification with molecular linkers; (4) Localized functionalization with probe molecules.

deposited on prefabricated SiNWs either by spin-coating or vapor-phase deposition. Second, an electrical current is passed through a SiNW for the localized Joule heating of the SiNW and subsequent ablation of the protective polymer layer. After a low power $O_2$ plasma treatment, the surface is modified with organic (e.g., organosilane) linkers for further biochemical functionalization. After an additional rinsing step, probe molecules are finally immobilized onto the chemical linkers that have been locally bound to the SiNW surfaces. This approach enables selective surface functionalization only along the SiNW while keeping the surrounding regions with a protective layer from being chemically modified.

Before the experimental demonstration, we first employed FEMLAB Multiphysics, a finite element analysis (FEA) program, to simulate the localized Joule heating in SiNWs. The simulation was based on an array of 10 single-crystalline p-type SiNWs (100 nm height, 100 nm width, 200 nm pitch, $5 \times 10^{18}/\text{cm}^3$ doping density) with a 30 nm thick polymer coating fabricated on a 400 nm thick silicon oxide ($SiO_2$) film on a p-type Si wafer. The detailed information about the numerical simulation is given in the Supporting Information. Accurate computation of nanoscale heat transfer in nanowires requires intensive modeling based upon molecular dynamics.[13] One-dimensional structures like nanowires have distinctive thermal and electric properties from their bulk material analogs. According to the literature,[14] these distinctions stem from several mechanisms such as quantum confinement, sharp features of one-dimensional density of states,[15] increased boundary scattering of electrons and phonons,[16] and modified electron−phonon and phonon−phonon scattering.[17,18] However, for the simplicity of the analysis, we only performed the numerical simulation based upon macroscale heat transfer models (e.g., Fourier law for heat conduction, Newton's law of convective cooling, Stefan−Boltzmann law of radiation, etc.) with bulk material properties.

For a single nanowire (no. 1) under an electrical bias of 2.5 V/$\mu$m (i.e., 10 V applied on a 4$\mu$m long SiNW), a maximum temperature of 599 K was observed from the simulation, as shown in Figure 2A. In addition, a very high temperature gradient was observed; temperatures dropped to 413 and 355 K for parallel wires only 200 and 400 nm away from the heated SiNW, respectively. This high-temperature gradient can be attributed to the small size of the heat source (SiNW) and thermal insulation by the underlying $SiO_2$ layer and air environment. For the case of four wires (nos. 1, 4, 7, and 10) under a simultaneous electrical bias of 3.0 V/$\mu$m (i.e., 12 V applied on 4$\mu$m long SiNWs), the temperature distribution is still localized on the chosen nanowires with a peak temperature of 812 K, as shown in Figure 2b. Although the temperatures of the neighboring nanowires also increase, they are still below 600 K. This large temperature gradient should allow a well-controlled selective ablation of the polymer coating from the heated SiNWs. The simulation excluded explicitly nanoscale heat transfer phenomena[18−20] and the phase changes of the polymer (evaporation or melting). The effective thermal conductivity of silicon can be reduced significantly for a nanowire of $<$100 nm in thickness or width due to the boundary phonon scattering effect.[14,18,20] Furthermore, the heating temperature of the SiNW will be even lower if the phase change of the polymer is considered because the phase change of the polymer is generally an endothermic process. Therefore, this analysis result may only provide a first-order approximation of the temperature distribution.

The nanoscale Joule heating of a SiNW and the consequent ablation of protective polymer was demonstrated with 50−100 nm wide, 50 nm thick, and 4−6 $\mu$m long SiNWs fabricated by a top-down approach. Briefly, the SiNW was made by electron beam lithography and reactive ion etching of a silicon on insulator (SOI) substrate with a thin Si device layer (50 nm thickness). The fabricated SiNWs had a linear current−voltage relationship, indicating an ohmic resistance of the SiNW and Si−Al contact. An average resistance of 562 k$\Omega$ was measured for 50 nm (W) $\times$ 50 nm (H) $\times$ 5 $\mu$m (L) SiNWs. A polytetrafluoroethylene (PTFE) thin film was used as the protective polymer layer, and 3-mercaptopropyltrimethoxysilane (3-MPTMS) was used as the chemical linker for selective surface functionalization of SiNWs. The detailed experimental procedure can be found in the Supporting Information.

AFM images of a single SiNW with the PTFE thin film coating before and after Joule heating are shown in Figure 3. A bias voltage of 30 V was applied across the SiNW in order to increase the temperature of the SiNW for the ablation of the PTFE film. The ablation occurred only in a very close proximity to the SiNW, while the surrounding regions were only slightly affected. A magnified AFM scan at the center of the SiNW shown in Figure 3c,d clearly indicates the local ablation of the PTFE film. This result verifies that highly localized Joule heating of SiNW did occur. The comparison

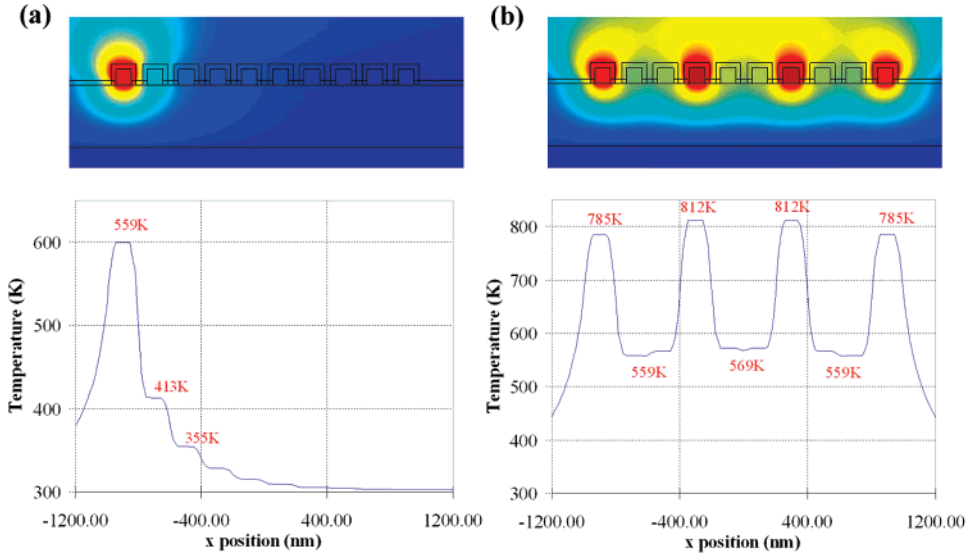


**Figure 2.** Numerical simulation results of temperature distribution in SiNW arrays by Joule heating through SiNW (a) heat applied only on nanowire no. 1 (left-most nanowire) by 10 V bias for 4 $\mu$m length, (b) heat applied on nanowires nos. 1, 4, 7, and 10 by 12 V bias for 4 $\mu$m length.

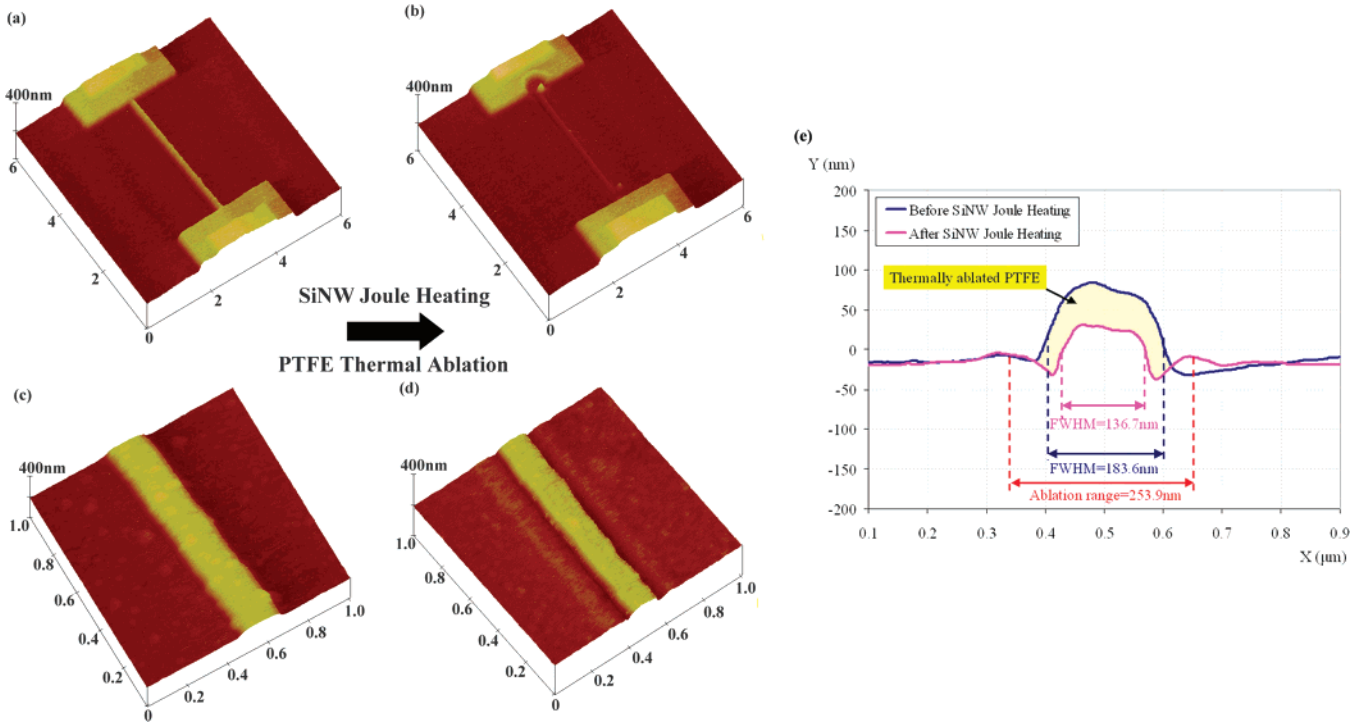


**Figure 3.** AFM images of localized ablation of PTFE thin films by nanoscale Joule heating along single SiNW (100 nm width, 50 nm height). (a,c) AFM image before SiNW Joule heating and polymer ablation. (b,d) AFM image after SiNW Joule heating and polymer ablation. (e) Cross-sectional profiles of SiNW before and after PTFE ablation by SiNW Joule heating. The discrepancy between two profiles indicates ablation of PTFE film by SiNW Joule heating.

of cross-sectional images before and after the SiNW Joule heating (see Figure 3e) provides quantitative information about the ablation of the PTFE film. Herein, blue and magenta lines represent the cross-sectional profiles of SiNWs with a PTFE film coating before and after Joule heating, respectively. The difference of these two profiles represents the ablated PTFE film. A step height reduction by ~40 nm indicates complete ablation of the PTFE film. The lateral range of PTFE ablation is measured as 254 nm. This indicates that the temperature rise occurred only close to the heated SiNW. From the measurement of electrical conductance, it is conjectured that the Joule heating and thermal ablation of PTFE film do not impact the structure and electrical performance of the SiNWs (refer to the Supporting Information for more detail).

Nanoscale Joule heating was also demonstrated in a high density array of SiNWs, as shown in Figure 4. An array of 11 SiNWs (50 nm width, 250 nm pitch) was fabricated and

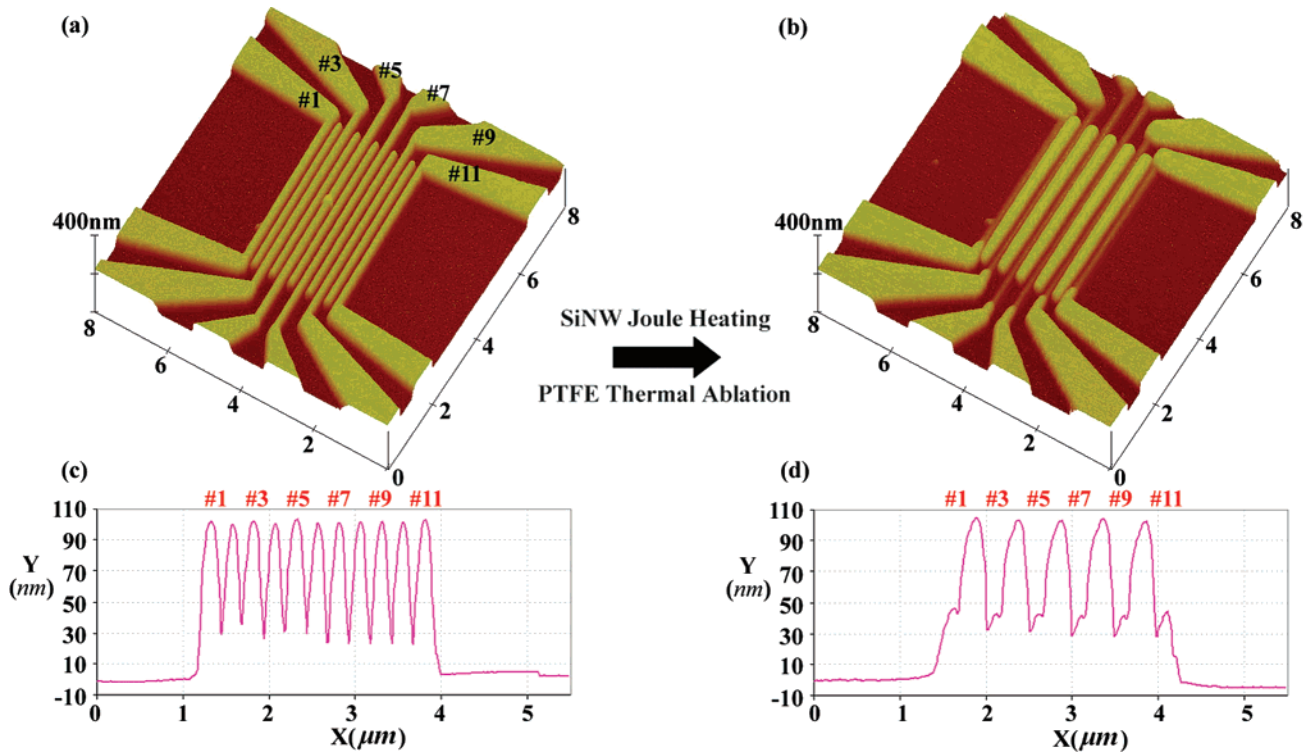


**Figure 4.** AFM images of a high-density SiNW arrays (50 nm width, 250 nm pitch) coated with 50 nm PTFE before (a) and after (b) the Joule heating. The cross-sectional profiles across the nanowire region are shown in (c) and (d) respectively. The ablation of PTFE occurred only along the chosen SiNWs (nos. 1, 3, 5, 7, 9, and 11) without significantly heating the neighboring SiNWs (nos. 2, 4, 6, 8, and 10).

coated with a 50 nm thick PTFE film. A bias voltage of 30 V was applied only on SiNW nos. 1, 3, 5, 7, 9, and 11 in series. The AFM images and cross-sectional profiles of the SiNW array show that the ablation of PTFE occurred only along the chosen SiNWs without significantly heating the neighboring SiNWs. The widths of unheated SiNWs nos. 2, 4, 6, 8, and 10 were found to be increased by 70−90 nm. This can be attributed to the PTFE reflow from the heated wires toward the unheated wires. The thermal conductivities of $SiO_2$ and air at room temperature are ~1.4 W/m·K and 0.03 W/m·K (for macroscale materials at room temperature), respectively. These values are lower than the thermal conductivity of single-crystalline silicon by several factors. The thermal insulation across the $SiO_2$ and air prevents the heat dissipation from SiNWs to the surrounding regions, facilitating the high-temperature rise of the SiNWs and the steep temperature drop in the surrounding areas. Consequently, localized nanoscale heating with high-temperature gradient (>1.5 K/nm from numerical simulation) is created by nanoscale Joule heating of a SiNW.

The change of the surface chemistry via thermal ablation of a protective polymer on a bare silicon surface was studied by water contact angle measurement, film thickness, and X-ray photoelectron spectroscopy (XPS). We prepared 1 × 1 $cm^2$ large Si substrates coated with PTFE thin films and tested their thermal ablation at different elevated temperatures for different durations on a hotplate. The thickness of the PTFE film and the surface water contact angle for a PTFE-coated Si substrate were 53 nm (from surface profilometry) and 112°, respectively, before starting the thermal ablation. For the sample heated at 813 K for 1 min, the film thickness was measured to be zero, while the contact angle was still measured to be 57°. This contact angle implies that there is some polymer residue on the ablated surface. Further treatment with low power (12 W) $O_2$ plasma for a short period (10 s) completely removed the residual species, and the contact angle reduced to <5°. This highly hydrophilic surface after the $O_2$ plasma treatment suggests that there were hydroxyl (−OH) groups on the silicon surface that are available for further attachment of chemical linker molecules, for example, 3-mercaptopropyltrimethoxysilane (3-MPTMS). We used a vapor-phase molecular assembly process to demonstrate the attachment of 3-MPTMS. After the process, the contact angle was measured to be 35.8°, indicating the successful surface modification with 3-MPTMS. Also, XPS analysis of this sample showed the presence of sulfur (S 2p) from 3-MPTMS linkers on the surface. On the other hand, for the sample heated at 673 K for 1 min, the film thickness was reduced to 12 nm, and the contact angle dropped a few degrees (112° → 106°). After $O_2$ plasma treatment, the water contact angle dropped to 22°, which suggested that the residual PTFE film is mostly etched by the $O_2$ plasma. For the sample heated at 573 K for 1 min, the PTFE film thickness only reduced 12 nm (53 → 41 nm) and the contact angle decreased 7° (113° → 106°). Because the PTFE film was barely ablated in this case, the thickness remained significant even after the $O_2$ plasma treatment and the surface remained hydrophobic with a water contact angle of 95.7°. XPS analysis of this sample treated with 3-MPTMS showed no peaks of sulfur (S 2p) and silicon (Si 2p), indicating that

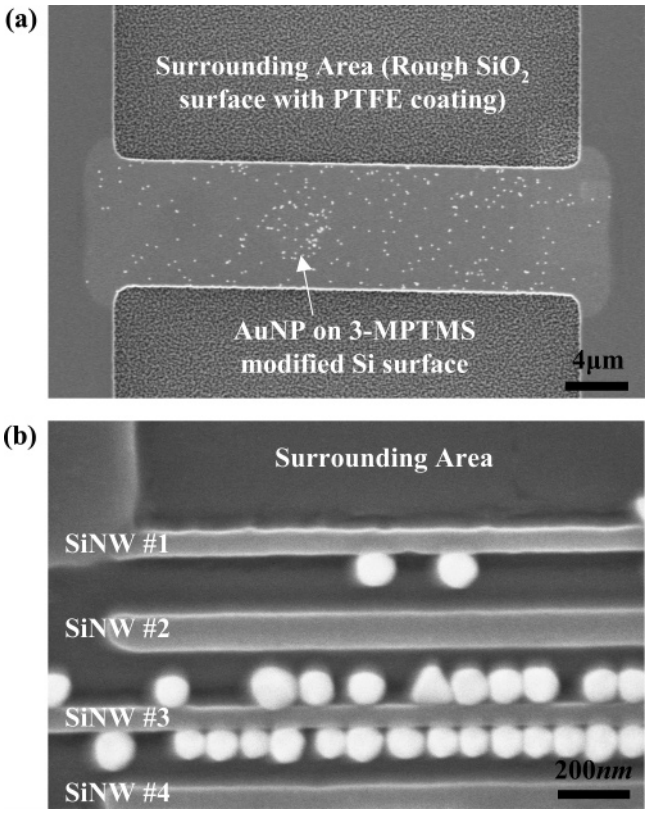


**Figure 5.** (a) Selective binding of gold nanoparticles on the surface of silicon microwire selectively functionalized with 3-MPTMS SAM layer. (b) Selective binding of gold nanoparticles on the high-density SiNW arrays. SiNW nos. 1 and 3 were treated by thermal ablation of PTFE and modified with 3-MPTMS SAM layer. SiNW nos. 2 and 4 were still protected by PTFE layer.

no 3-MPTMS linkers were attached on the PTFE surface. Figures S3 and S4 in the Supporting Information summarizes these results.

After selective removal of a PTFE film by localized Joule heating and low power $O_2$ plasma treatment, we functionalized the SiNW surface with 3-MPTMS by vapor-phase deposition. This particular molecule is a common linker for the attachment of protein or DNA molecules. The thiol (−SH) terminal group in the molecules also has a strong affinity to bind to gold. Because of this reason, we decided to use gold nanoparticles to visualize that the 3-MPTMS was indeed selectively bound to SiNW, not on the surrounding regions covered with PTFE. After thorough rinsing with deionized water and isopropyl alcohol (IPA) for the removal of nonspecifically bound 3-MPTMS groups on the PTFE film, we dispensed a solution of gold nanoparticles (AuNP, 100 nm diameter, Ted Pella, Inc.) on the sample surface. After storing at room temperature for 2 h in a small container that is hydrated and tightly sealed, and additional rinsing with DI water and IPA, we could observe that AuNPs were selectively bound to the surface of the Joule-heated samples as shown in Figure 5. In Figure 5a, selective surface functionalization was performed on the microscale silicon wires (8 $\mu$m wide, 32 $\mu$m long). The PTFE film was selectively ablated along the silicon microwire onto which 3-MPTMS was attached. As shown in this figure, the AuNPs were bound only on the surface of silicon wire but not on the surrounding regions covered with PTFE film. In Figure 5b, selective surface functionalization was demonstrated on the high-density SiNWs (50 nm width, 250 nm pitch). The surfaces of SiNW nos. 1 and 3 were exposed by thermal ablation via nanoscale Joule heating while the SiNWs nos. 2 and 4 were still protected by the PTFE film. The difference in the line width shown in the figure is due to the thickness of the PTFE coating around SiNW no. 2. As shown in the figure, AuNPs were bound only on the surface of SiNW nos. 1 and 3 (surface exposed and functionalized with 3-MPTMS), not on the SiNW nos. 2 and 4. Although only three AuNPs were bound on SiNW no. 1, SiNW no. 3 was densely packed with more than 20 AuNPs. Also, no AuNPs were found on the surrounding area. This experimental result verifies that the surface of the SiNWs nos. 1 and 3 was selectively functionalized with 3-MPTMS.

In summary, we have developed a novel method for selective surface functionalization of SiNWs by thermal ablation of protective polymer layers with self-aligned local Joule heating of SiNWs. This thermal ablation is followed by an $O_2$ plasma cleaning step before subsequent functionalization by an organosilane linker. We have then successfully visualized the selective surface modification of a SiNW surface with 3-MPTMS by using gold nanoparticles. It is conceivable that this localized joule heating approach can be generalized to many polymers that can undergo either chemical decomposition or physical ablation under elevated temperatures. Therefore, we expect that the selective surface functionalization approach we developed here will be extremely valuable for nanowire-based sensor development as well as other MEMS/NEMS applications that require localized surface engineering. Furthermore, we believe that this approach will not only work for SiNWs, but also for other semiconducting or metallic nanostructures that have two terminals for electrical addressing.

**Acknowledgment.** We thank Dr. William Flounders at the Berkeley Sensor and Actuator Center (BSAC), University of California, Berkeley, and Dr. Eung-Sug Lee at Korea Institute of Machinery and Materials for valuable discussions. Also, we thank the staff at Microfabrication Laboratory at UC Berkeley and Xuema Li at Hewlett-Packard (HP) Laboratories, Palo Alto, CA, for help with device fabrication. Financial support by the Center for Nanoscale Mechatronics and Manufacturing (grant no. 019997), one of the 21st Century Frontier Research Programs from the Ministry of Science and Technology, Republic of Korea, is gratefully acknowledged. Partial support was also supplied by Hewlett-Packard (HP) Laboratories.

**Supporting Information Available:** Synthetic procedures and device fabrication methods. This material is available free of charge via the Internet at http://pubs.acs.org.

## References

(1) Cui, Y.; Wei, Q.; Park, H.; Lieber, C. M. *Science* **2001**, *293*, 1289−1292.
(2) Zhou, X. T.; Hu, J. Q.; Li, C. P.; Ma, D. D.; Lee, C. S.; Lee, S. T. *Chem. Phys. Lett.* **2003**, *369*, 220−224.

(3) Li, Z.; Chen, Y.; Li, X.; Kamins, T. I.; Nauka, K.; Williams, R. S. *Nano. Lett.* **2004**, *4*, 245−247.
(4) Zheng, G.; Patolsky, F.; Cui, Y.; Wang, W. U.; Lieber, C. M. *Nat. Biotechnol.* **2005**, *23*, 1294−1301.
(5) Patolsky, F.; Timko, B. P.; Yu, G.; Fang, Y.; Greytak, A. B.; Zheng, G.; Lieber, C. M. *Science* **2006**, *313*, 1100−1104.
(6) Park, I.; Li, Z.; Li, X.; Pisano, A. P.; Williams, R. S. *Biosens. Bioelectron.* **2007**, *22*, 2065−2070.
(7) Hahm, J.; Lieber, C. M. *Nano Lett.* **2004**, *4*, 51−54.
(8) Naujoks, N.; Stemmer, A. *Microelectron. Eng.* **2003**, *67*−*68*, 736−741.
(9) Lee, C.-S.; Lee, S.-H.; Park, S.-S.; Kim, Y.-K.; Kim, B.-G. *Biosens. Bioelectron.* **2003**, *18*, 437−444.
(10) Renault, J. P.; Bernard, A.; Juncker, D.; Michel, B.; Bosshard, H. R.; Delamarche, E. *Angew. Chem., Int. Ed.* **2002**, *41*, 2320−2323.
(11) Lim, J.-H.; Ginger, D. S.; Lee, K.-B.; Heo, J.; Nam, J.-M.; Mirkin, C. A. *Angew. Chem., Int. Ed.* **2003**, *115*, 2411−2414.
(12) Bunimovich, Y.; Ge, G.; Ries, R.; Beverly, K.; Hood, L.; Heath, J. *Langmuir* **2004**, *20*, 10630−10638.
(13) McConnell, A. D.; Goodson, K. E. *Annu. Rev. Heat Trans.* **2005**, *14*, 129−168.
(14) Zhang, Y.; Christofferson, J.; Shakouri, A.; Li, D.; Majumdar, A.; Wu, Y.; Fan, R.; Yang, P. *IEEE Trans. Nanotechnol.* **2006**, *5*, 67−74.
(15) Lin, Y.-M.; Sun, X.; Dresselhaus, M. S. *Phys. Rev. B* **2000**, *62*, 4610−4623.
(16) Zou, J.; Balandin, A. *J. Appl. Phys.* **2001**, *89*, 2932−2938.
(17) Li, D.; Wu, Y.; Fan, R.; Yang, P.; Majumdar, A. *Appl. Phys. Lett.* **2003**, *83*, 3186−88.
(18) Chen, Y.; Li, D.; Lukes, J. R.; Majumdar, A. *J. Heat Trans.* **2005**, *127*, 1129−1137.
(19) Li, D.; Wu, Y.; Kim, P.; Shi, L.; Yang, P.; Majumdar, A. *Appl. Phys. Lett.* **2003**, *83*, 2934−2936.
(20) Ju, Y. S.; Goodson, K. E. *Appl. Phys. Lett.* **1999**, *74*, 3005−3007.

NL071637K